



# Evaluation of RTM and models for MW and IR all-sky assimilation

Yoshifumi Ota, Kozo Okamoto and Masahiro Kazumori  
Japan Meteorological Agency (JMA)

2019 International Workshop on Radiative Transfer Models for Satellite Data Assimilation,  
Tianjin, 29 April – 2 May, 2019

# Contents

## Recent research activities regarding radiative transfer model (RTM) in JMA

1. All-sky assimilation of microwave (MW) radiation data
2. All-sky assimilation of infrared (IR) radiation data
3. Development of adjoint radiative transfer model including scattering effect

# 1. All-sky assimilation of microwave (MW) radiation data

# Introduction

- ◆ Microwave (MW) brightness temperature (BT) data is essential to keep and improve accuracy of numerical prediction system (NWP).
- ◆ Using MW BT of satellite observation, atmospheric information of temperature, water vapor, cloud, and precipitation is obtainable **at cloud area**.
- ◆ JMA is developing the global data assimilation system that **uses the MW BT data at all-sky condition including cloud/precipitation areas**.
- ◆ Generally, in the framework of data assimilation that analyzes the initial values for NWP, **both observation and model calculation are required to have no bias errors**.

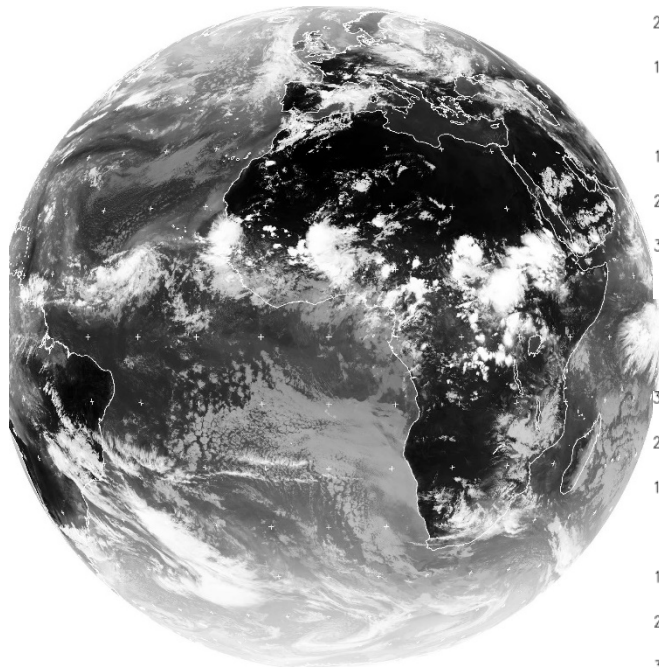
# Forecast model bias issues in all-sky MW DA

Underestimation of strong convective clouds in the JMA global model?

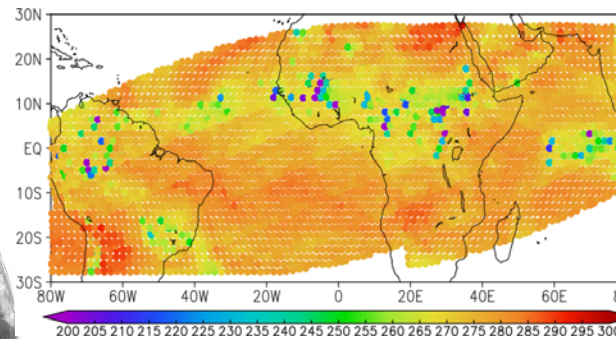
SAPHIR 183.31+6.8 GHz

August 14, 2016 (all-sky passive)

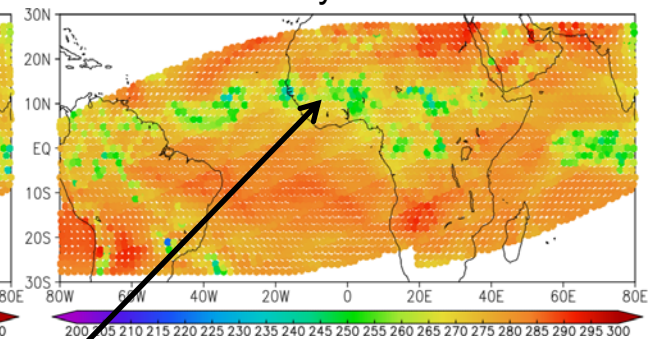
Meteosat-10 IR



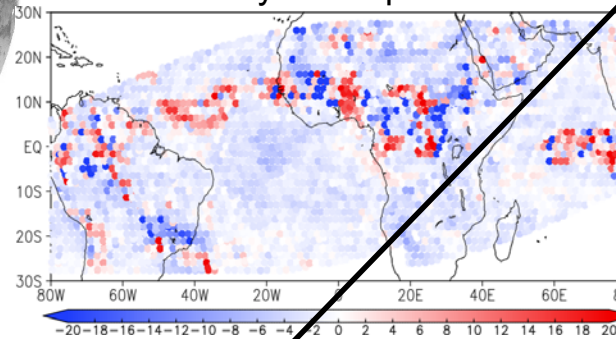
Observed BT



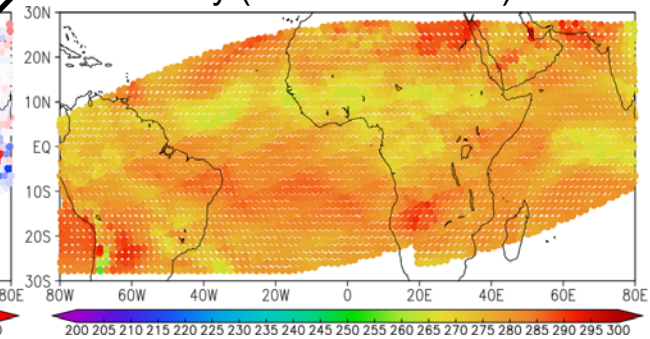
All-sky FG BT



All-sky FG departure



Clear-sky (w/o cloud effect) FG BT



Model's convective clouds are weak and broadly spread.

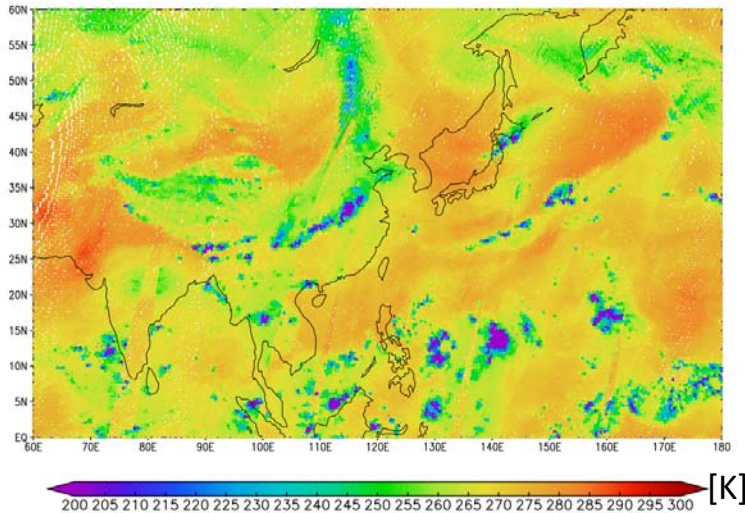
Model's precipitation representation is crucial for all-sky 183 GHz humidity sounding radiance assimilation.

# Objective and method

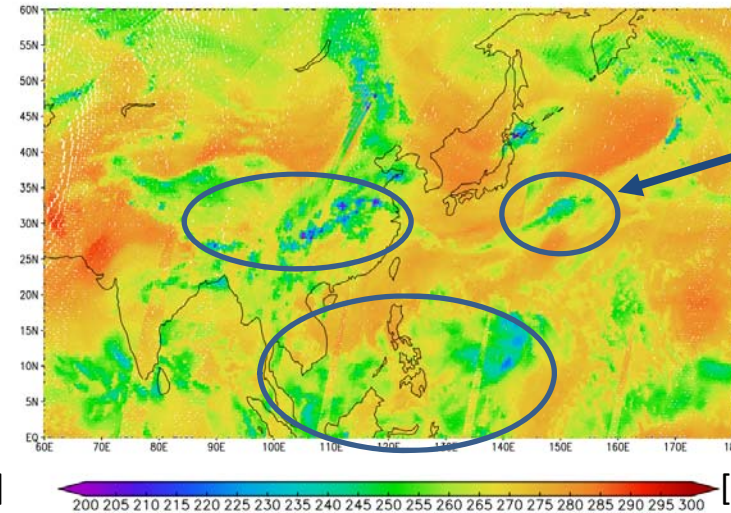
- ◆ By comparing observation and calculation of BT, investigation of the characteristics and bias errors of JMA's Global Spectral Model (GSM) at cloud/precipitation areas where effects of cloud, rain, and snow are significant
- ◆ Simulations of MW BT at the cloud/precipitation areas using RTTOV v10.2 (RTTOV\_SCATT) with input profiles of cloud, rain, and snow from GSM

# MHS: Comparison of spatial distribution of BT

Obs. BT  $183.31 \pm 7$  GHz

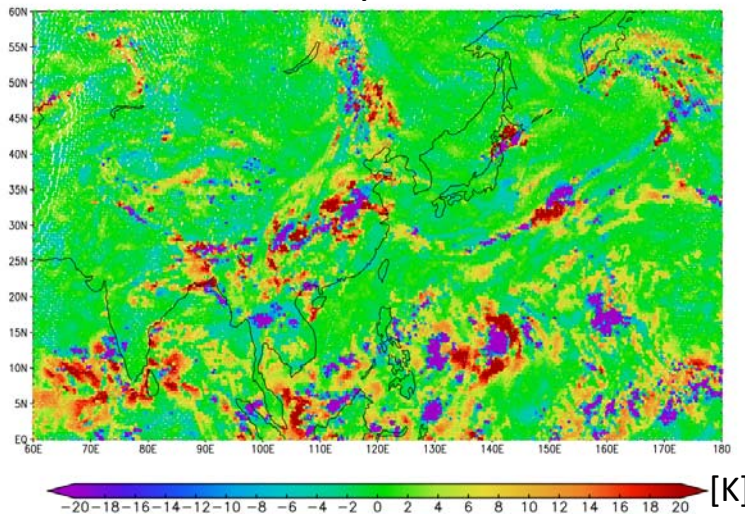


Calc. BT (RTTOV\_SCATT default setting)

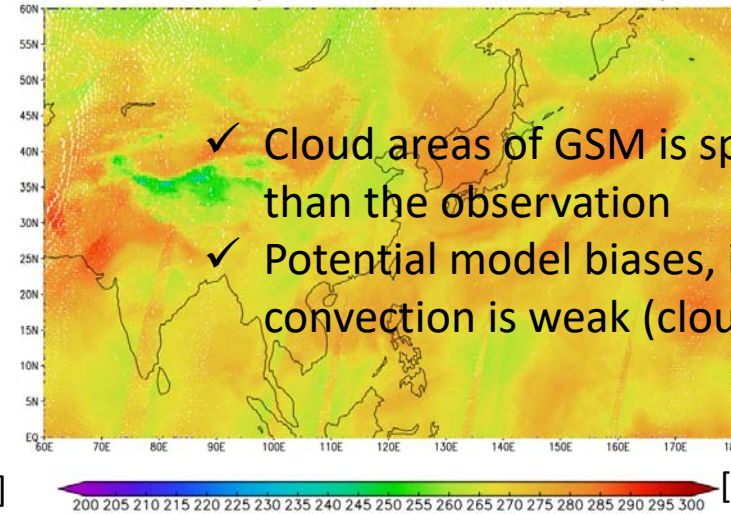


Cloud areas

FG departure



Calc. BT (without cloud effect)



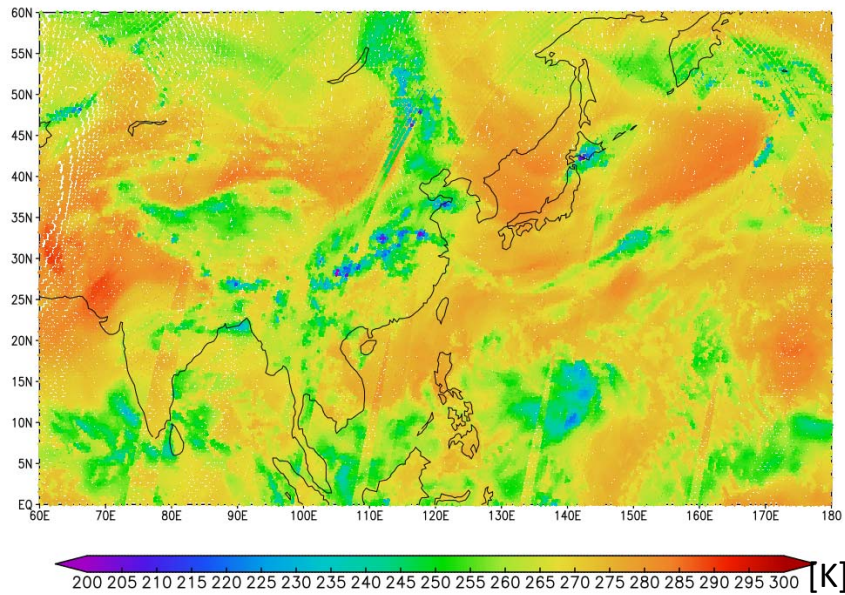
- ✓ Cloud areas of GSM is spatially-smoother than the observation
- ✓ Potential model biases, i.e. effect of deep convection is weak (cloud-top is low)

00 UTC, 10 Sep. 2017

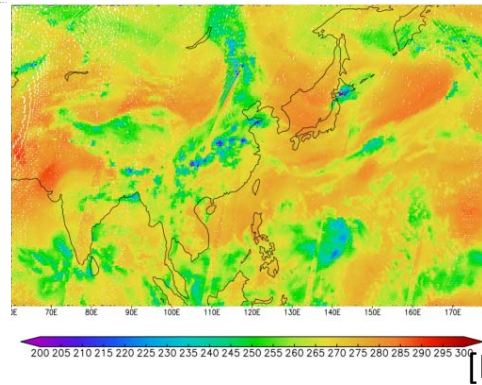
# Effect of hydrometers that are input to RTM

Experiment to see BT differences by zeroing input profile values of water/ice cloud, rain, and snow for RTM

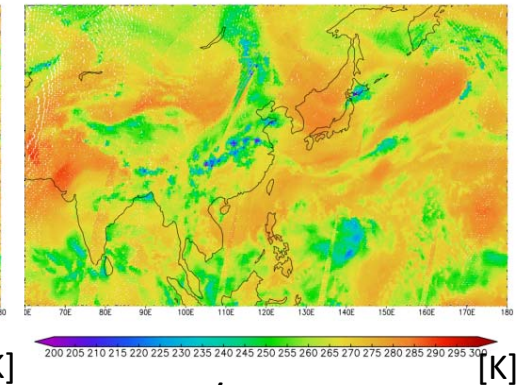
MHS Ch 5. ( $183.31 \pm 7$  GHz)  
Calc. BT



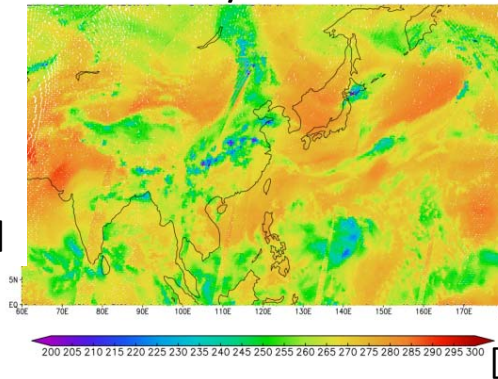
w/o water cloud



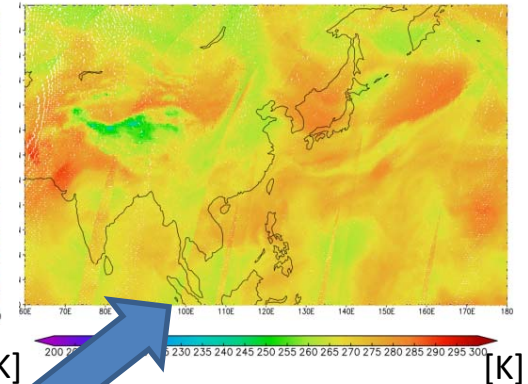
w/o ice cloud



w/o rain



w/o snow



**Scattering effect by snow has significant decrease in BT.**

00 UTC, 10 Sep. 2017



# Shape of ice crystals implemented in RTTOV\_SCATT

11 types

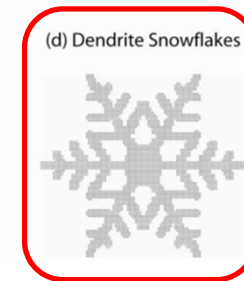
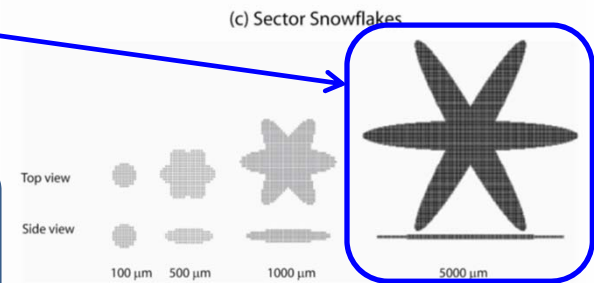
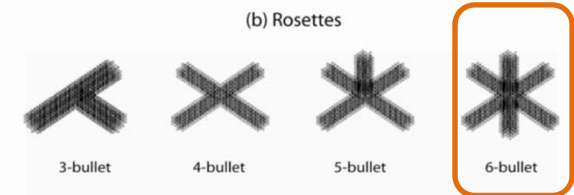
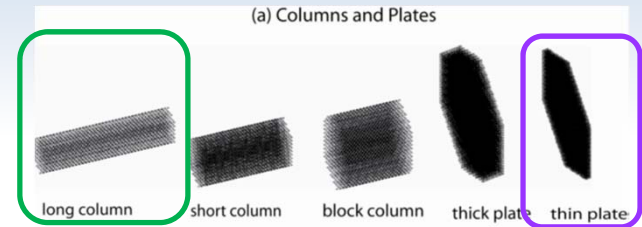
- long column
- short column
- block column
- thick plate
- thin plate
- 3-bullet rosette
- 4-bullet rosette
- 5-bullet rosette
- 6-bullet rosette
- sector snowflake
- dendrite snowflake

- Only bulk process of cloud physics is implemented in GSM.
- In RTM, one snowflake model has to be specified as a representative that is consistent globally with satellite observation.

Default setting of RTTOV\_SCATT  
Used in NWP system of ECMWF

- Optical property of hydrometers (LUT at frequency, temperature, and mass)
  - Water/Ice cloud    Mie Sphere, Gamma PSD
  - Rain                    Mie Sphere, Marshall-Palmer PSD
  - Snow                    Liu et al. (2008) snowflake, Field et al. (2007) PSD
  - Cloud fraction        Beam-filling, sub-grid cloud overlap    Geer et al. (2009)
- Input atmospheric profiles from GSM (FT = 3 ~ 9hr)

T, q, O<sub>3</sub>, Q<sub>c</sub>, Q<sub>i</sub>, Q<sub>rain</sub>, Q<sub>snow</sub>, Q<sub>frac</sub>

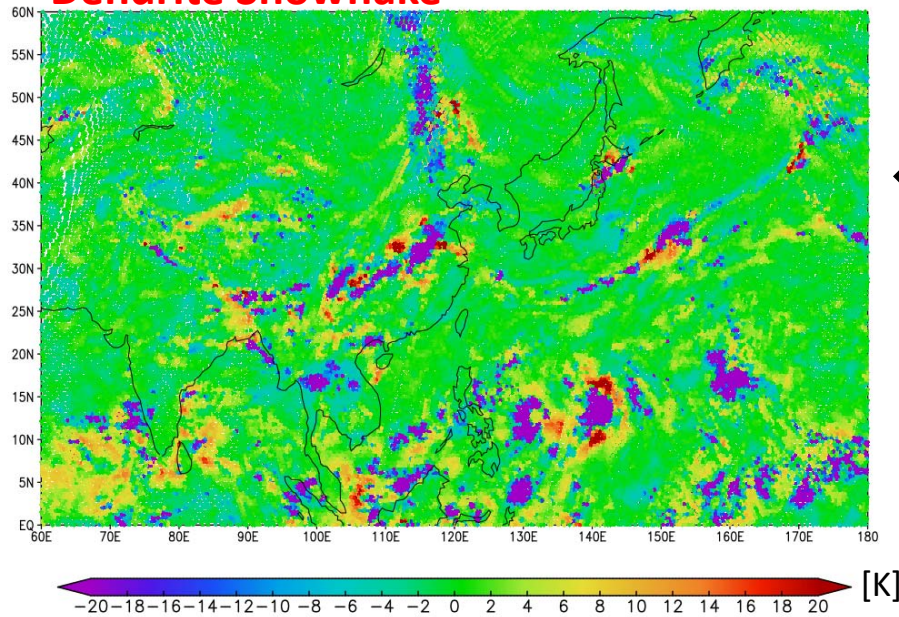


Liu et al. (2008)

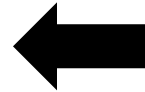
# Comparison of horizontal distribution of FG departure of MHS Ch 5. ( $183.31 \pm 7$ GHz)

FG departure = Observation – First guess (FG)

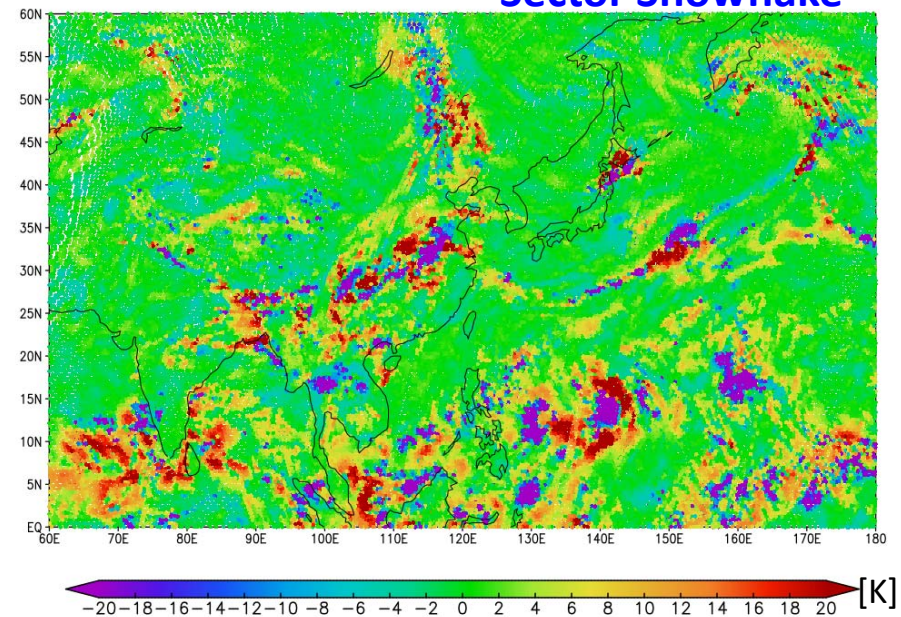
### Dendrite Snowflake



By using different snowflake model, the positive biases around cumulus cloud decreases but the negative biases still remain in the deep convective area.



### Sector Snowflake



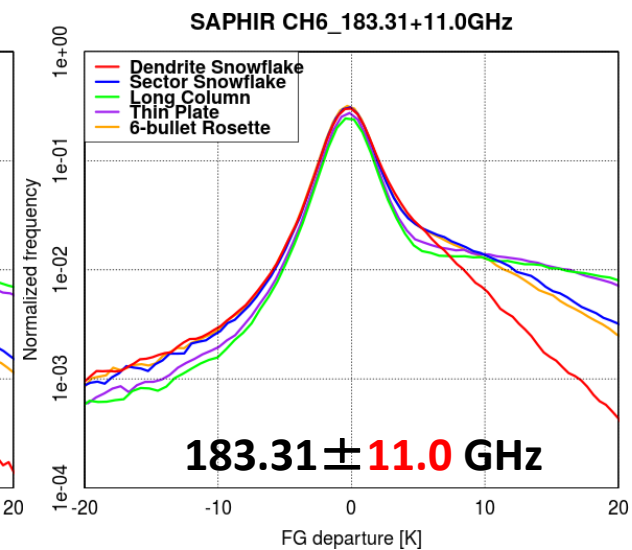
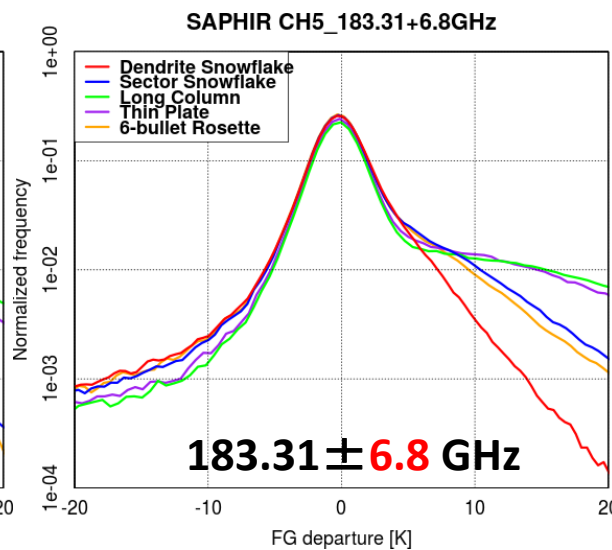
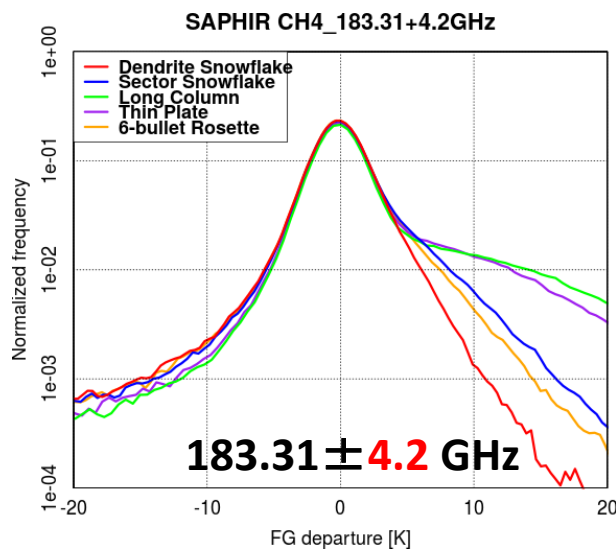
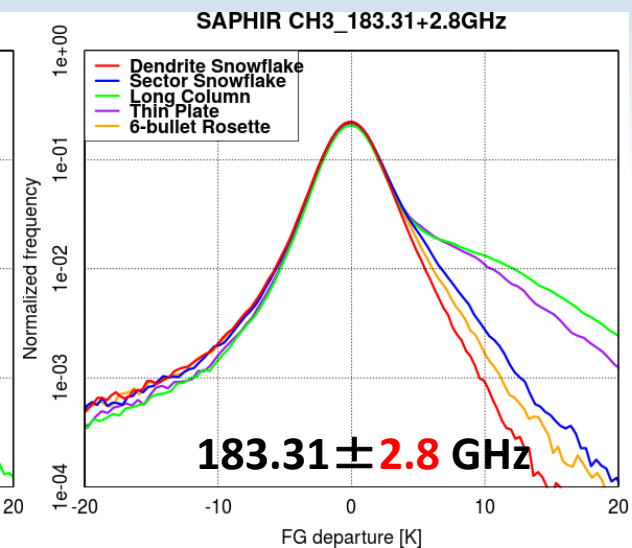
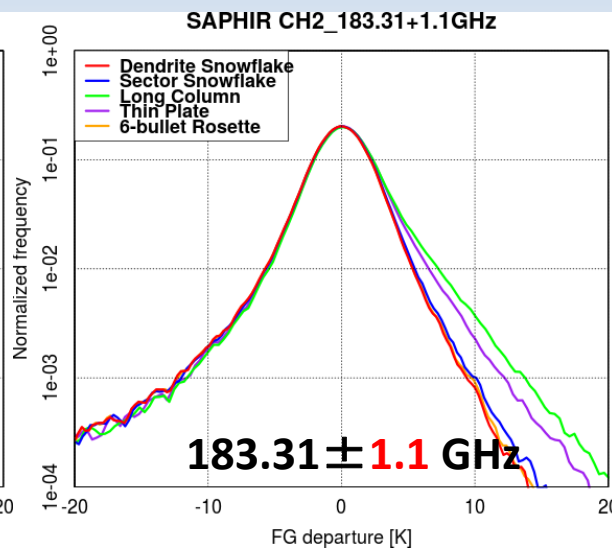
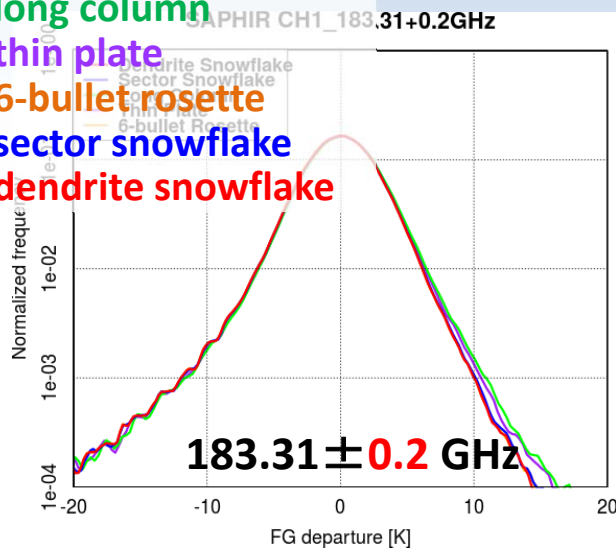
Calculation is adjustable to be the observation by tuning observation operator but is it valid?  
(Input profiles from GSM has also model biases.)

Can a single shape model of snowflake be the representative?

Actually, some types are mixed depending on temperature & ice saturation.

# Histogram of FG departure (difference between Obs. and Calc. BT) Channel of MW sounder SAPHIR (difference in altitude)

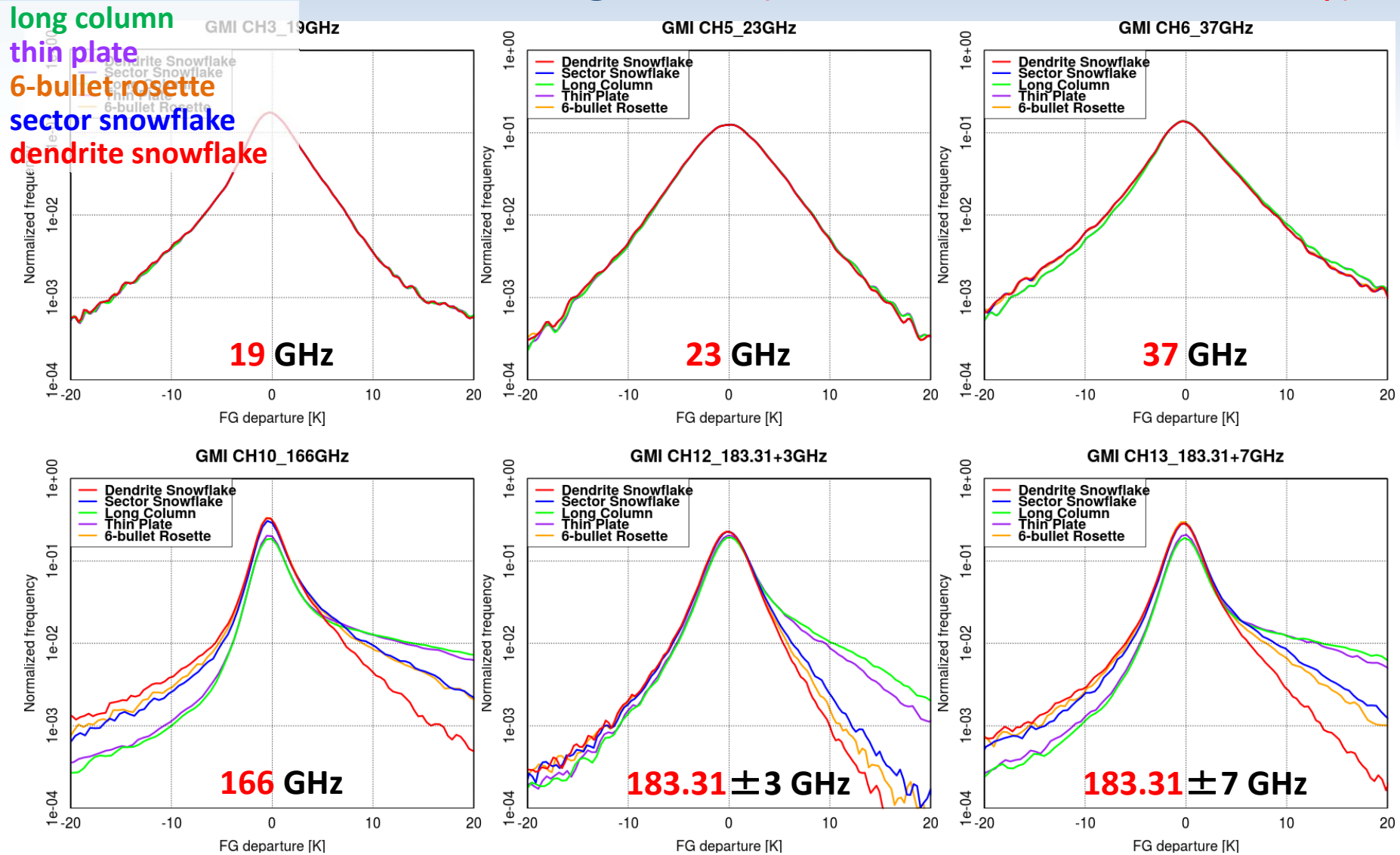
long column  
thin plate  
6-bullet rosette  
sector snowflake  
dendrite snowflake



Number of positive-biased data increases with the wider band (low altitude).

The biases depends on the shape model.

# Histogram of FG departure (difference between Obs. and Calc. BT) Channel of GPM MW imager GMI (difference in snow sensitivity)



Only high frequency channels sensitive to snow are affected by shape model.  
The result is trivial, but a single shape model cannot simulate the observation.



# Summary of topic 1

- ◆ Comparison of **MW observation and calculation BT on all-sky condition** using JMA's GSM in order to investigate model characteristics and biases.
- ◆ The GSM simulates convective clouds spatially-smoother than satellite observation. **FG departure (obs. – calc.) of BT has positive bias indicating potential model biases.**
- ◆ Using RTTOV-SCATT, experiment to see BT differences by changing input of hydrometers.
  - **Effect of snow is significant** at high frequency MW channels.
  - By using dendrite snowflake model, spatial distribution of BT differences (positive bias) decrease, but the differences at the area where cloud top is high did not improve.
- ◆ Input profiles (water/ice cloud, rain, and snow) from GSM to RTM affect calculation results of BT. However, **the representation of snowflake model also significantly affects the calculations.** Current RTM handles RT calculations for a single snowflake model as a representative.

## 2. All-sky assimilation of infrared (IR) radiation data

# Objective

- ◆ All-sky IR assimilation
  - Effectively assimilate IR cloud-affected satellite data to improve analysis and forecast
    - higher horizontal/vertical/temporal resolution
- ◆ Evaluate the operational global data assimilation system in all-sky condition
  - Compare observation and simulations to better understand their characteristics
  - Use RTTOV and Joint Simulator for Himawari-8

# Comparison of simulation and observation

## ◆ Simulations

- Model: Global Spectral Model (GSM)
  - 20 km res.
  - Initial: 06 UTC 9 Sep 2017, 6-h forecast
- Simulators (FG)
  - Joint-Simulator (JS)
  - RTTOV v10.2 (RT)

## ◆ Observations (OB)

- Himawari-8/AHI: IR radiances at 12 UTC 9 Sep 2017
  - Super-obs. (16x16 pixels average)
    - 120km thinning
  - Band 8 (6.2 $\mu$ m): water vapor (WV) band
  - Band 13 (10.4 $\mu$ m): window band



# Model and RTMs

## ◆ Global Spectral Model (GSM)

- Convection: Arakawa-Schubert
- Cloud: Smith(PDF) + diagnostic stratospheric cloud
- Hydrometeors: total cloud (liquid+ice), rain flux, snow flux

## ◆ RTTOV v10.2 (RT: Saunders et al. 2012, Hocking et al. 2018)

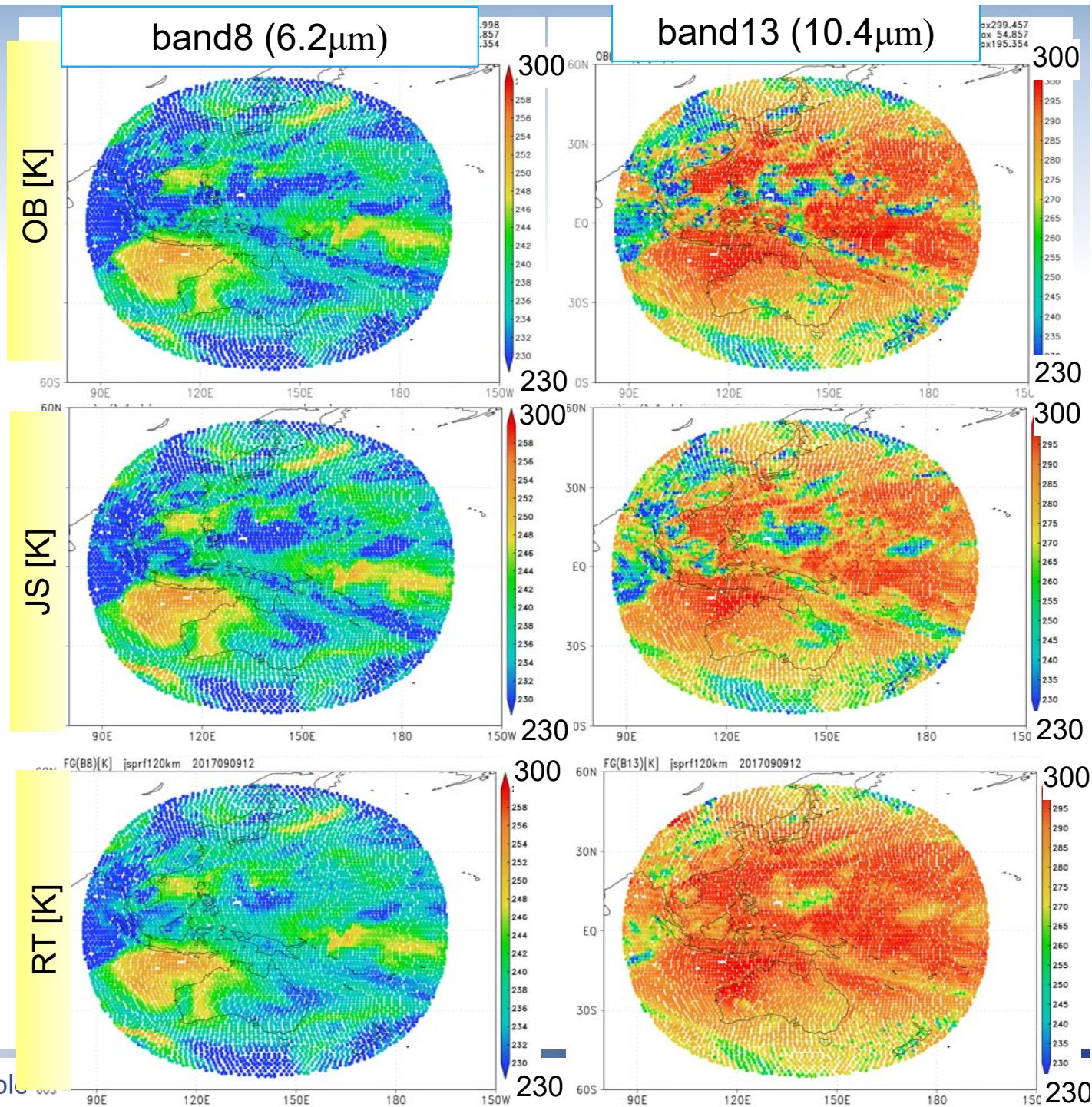
- Widely used in operational DA systems
  - fully evaluated in clear-sky conditions
- Cloud scattering: scaling approx. (Chou et al. 1999, J.Clim)
- Hydrometeor input: liquid cloud (5 type), ice cloud, and cloud fraction
  - No explicit input on PSD and  $V_t$ .
  - Ice: Set diameter from Wyser et al. (2010) and Hexagonal shape

## ◆ Joint-Simulator (JS: Hashino et al. 2013, JGR)

- Cloud scattering: DOM/adding (Nakajima & Tanaka 1986,1988, JQSRT)
- Hydrometeor input: mix.ratio of liq. cloud, ice cloud, rain, and snow, and cloud fraction

# OB,FG

◆ 20170909.  
12UTC



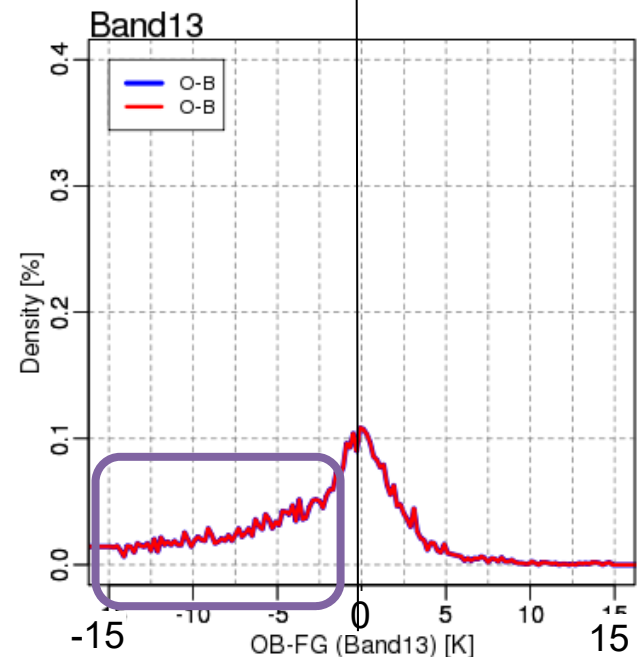
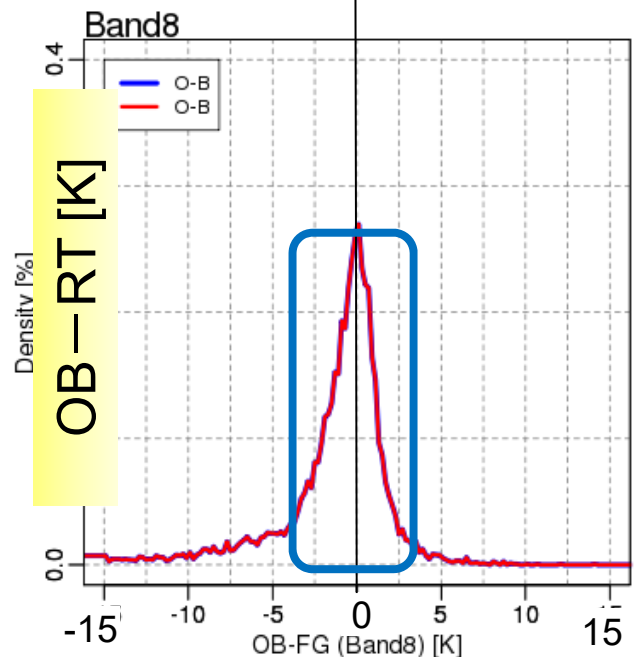
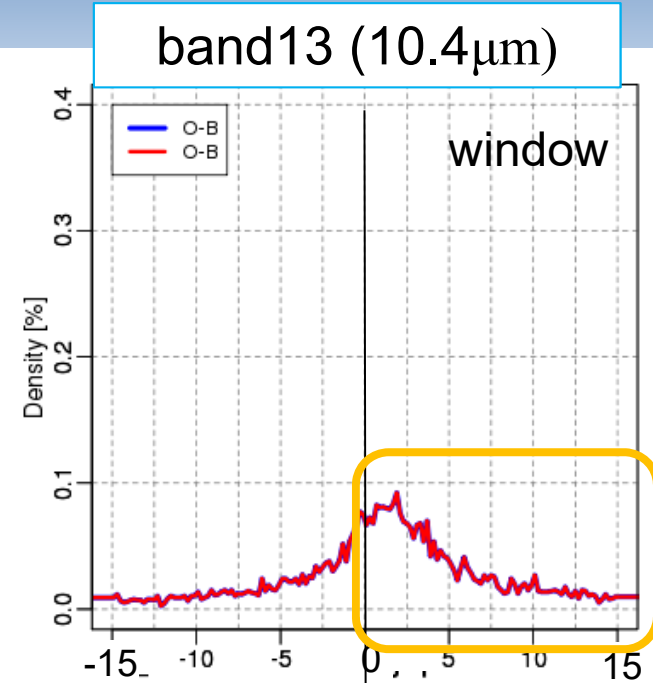
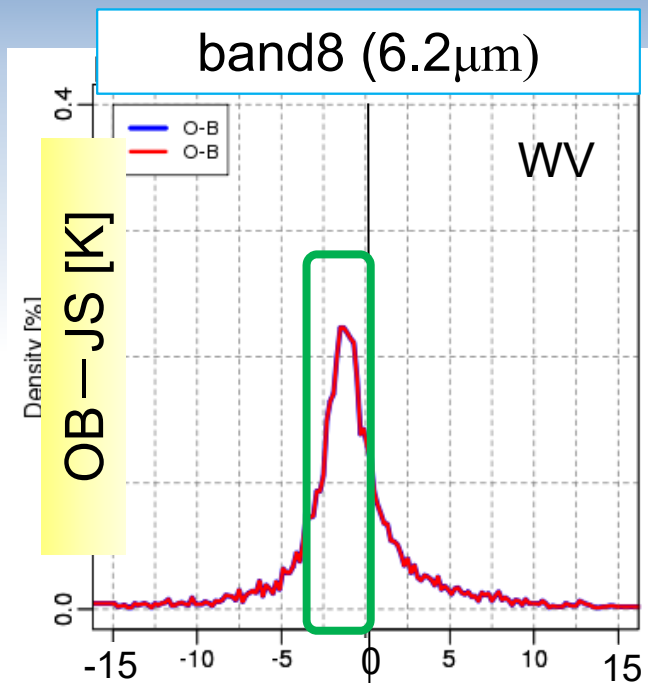
# OB-FG

- JS(b8) :  $OB-FG < 0$   
← WV abs. in JS ↓
- RT(b8) :  $OB-FG \sim 0$   
← looks good

- JS(b13) :  
 $OB-FG > 0$   
← cloud effect ↑

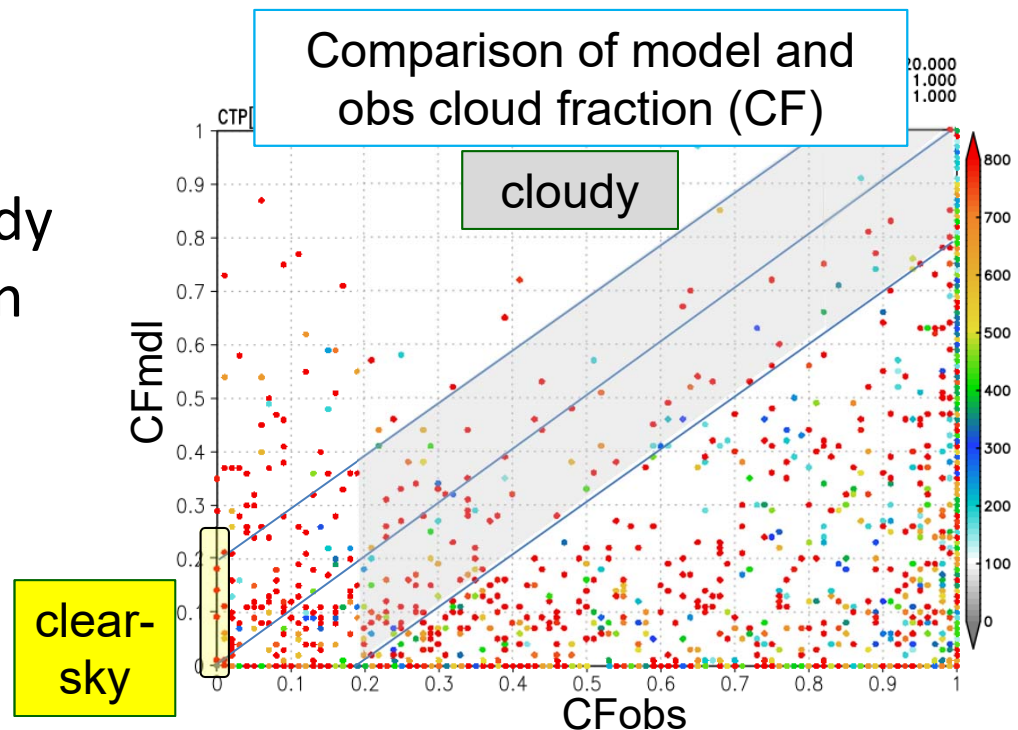
- RT(b13) :  
 $OB-FG < 0$   
← cloud effect ↓

- GSM clouds are underestimated



# Avoid the model bias

- ❑ Model underestimate upper and middle cloud
- ❑ Chose samples with consistent cloud between model and obs.
  - CFobs: cloud fraction (CF) from observation
  - CFmdl: model cloud fraction near observed cloud top height
  - $|CF_{obs}-CF_{mdl}| < 0.2$
- ❑ Classify into clear-sky or cloudy using observed cloud fraction
  - $CF_{obs}=0.0$  or  $CF_{obs}>0.2$



# clear-sky

## OB-FG

□ JS(b8): OB-FG < 0

← WV abs. ↓

□ RT(b8): OB-FG > ~0

← WV abs. ↑~

□ JS,RT(b13):

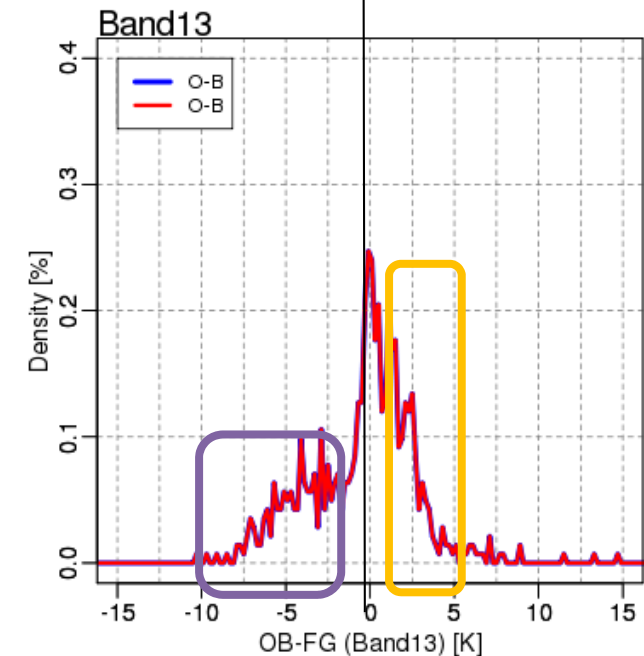
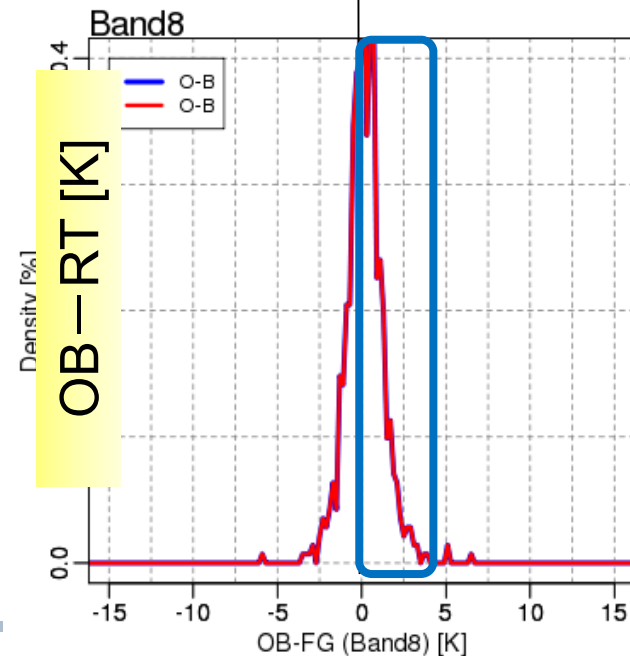
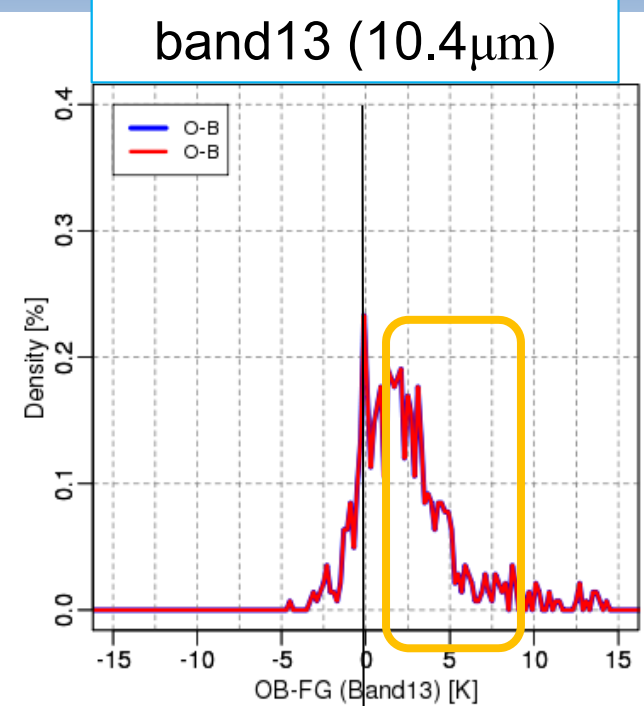
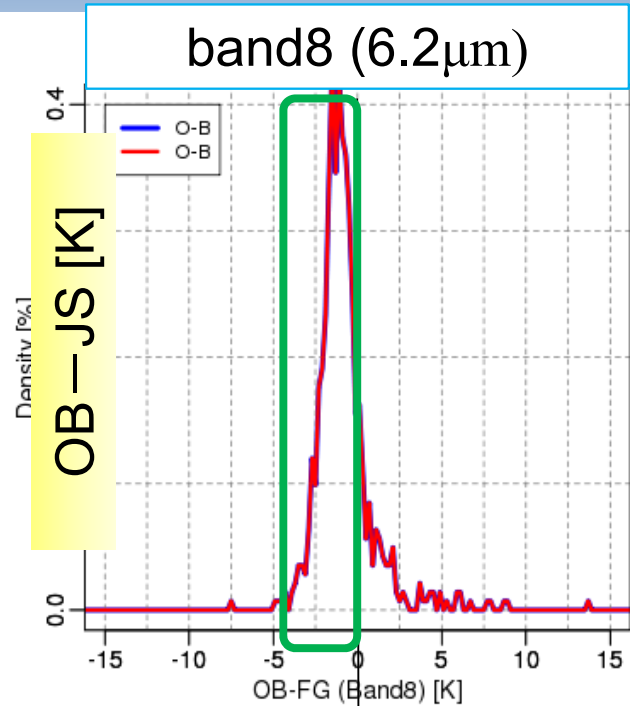
OB-FG > 0

← spurious model  
thin cloud?

□ RT(b13): OB-FG < 0

← land surface ↑

←  $T_s$  or  $\epsilon$  ↑



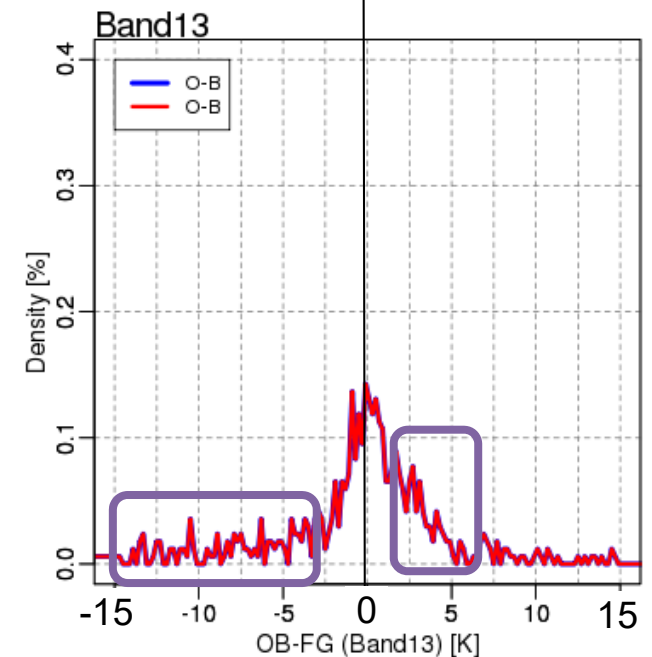
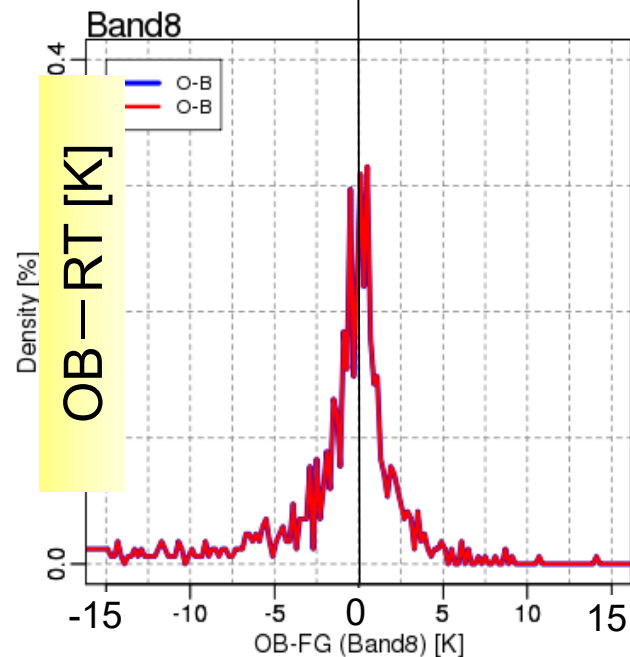
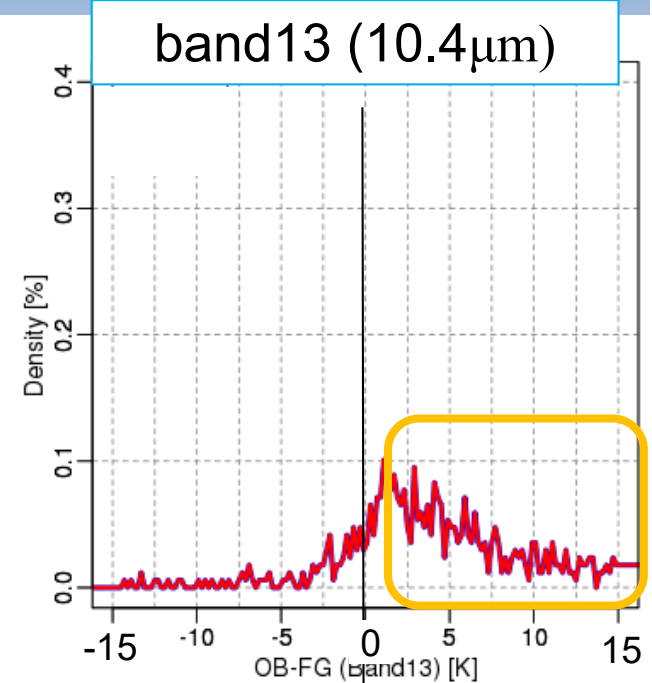
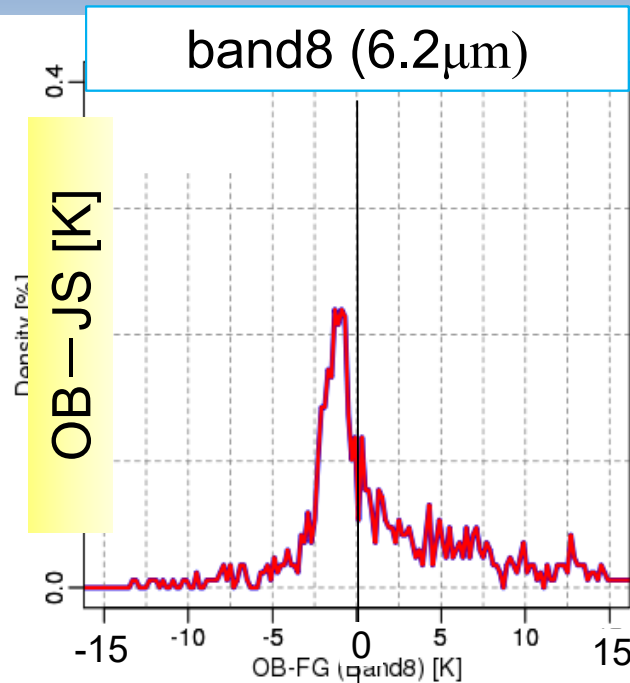
O-B : 708 a0.19 s1.12 x6.44 r-5.99 m-0.10 s0.23 k6.61  
O-B : 708 a0.19 s1.12 x6.44 r-5.99 m-0.10 s0.23 k6.61

O-B : 708 a-0.44 s3.14 x14.78 r-10.36 m-0.30 s0.00 k4.40  
O-B : 708 a-0.44 s3.14 x14.78 r-10.36 m-0.30 s0.00 k4.40

# cloudy OB-FG

□ JS(b13):  
OB-JS > 0 ←  
cloud effect in JS ↑

□ RT(b13):  
OB-FG > 0 ←  
liq. cloud effect ↑  
OB-FG < 0 ←  
ice cloud effect ↓

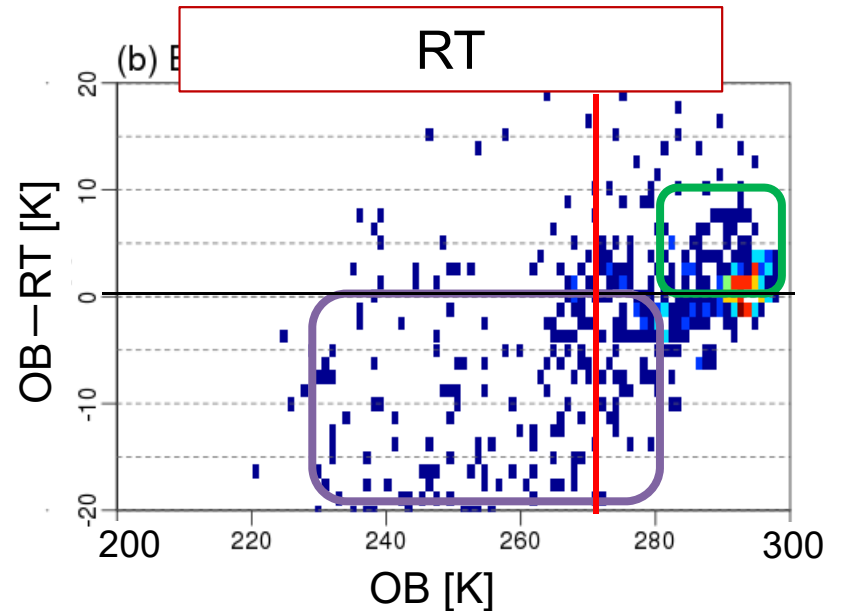
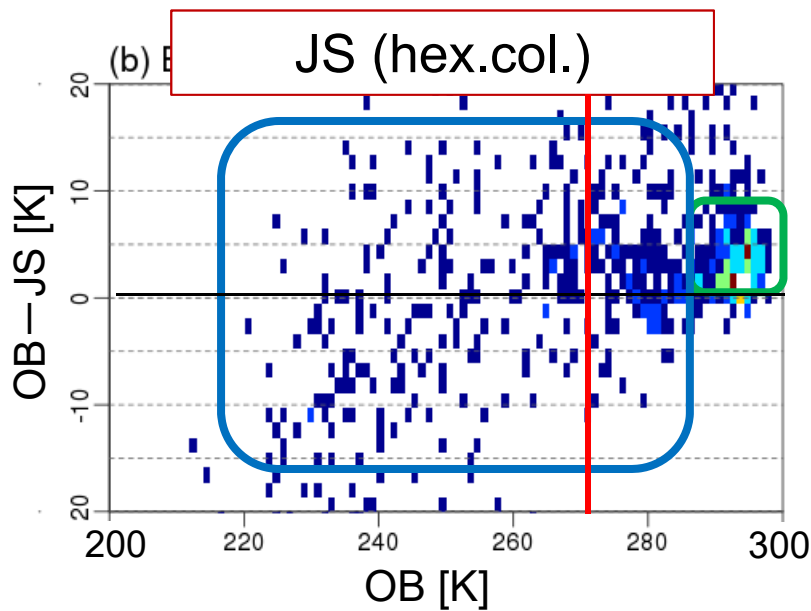
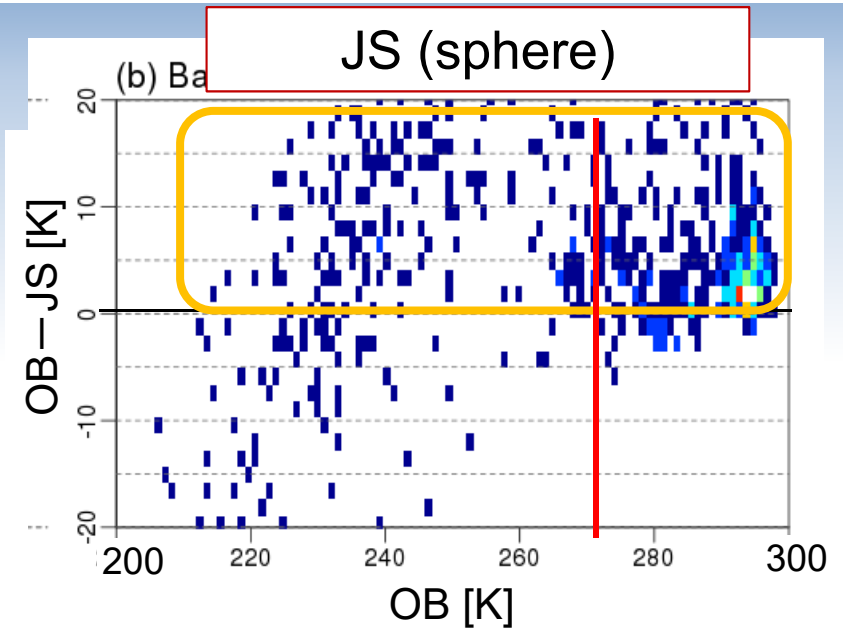


O-B :841 a-2.03 s5.74 x14.08 r-41.27 m0.30 s-2.25 k9.76  
O-B :841 a-2.03 s5.74 x14.08 r-41.27 m0.30 s-2.25 k9.76

O-B :841 a-9.47 s18.92 x32.24 r-94.00 m-0.30 s-1.56 k5.18  
O-B :841 a-9.47 s18.92 x32.24 r-94.00 m-0.30 s-1.56 k5.18

# OB vs OB-FG (cloudy, band13)

- JS: cloud ext. ↑
- RT: liq. cloud abs ↑  
ice cloud ext. ↓
- JS\_hexagonal column: ice cloud ext. lessens



# Summary of topic 2

- ◆ Evaluate global data assimilation system
  - Comparison of RT and JS reveals problems with
    - JS: Overestimate cloud effect and underestimate WV abs.  
Hex. col. ice alleviates the overestimation
    - RT: Underestimate ice cloud effect and  
Overestimate liq. cloud effect and WV abs.
- ◆ Further investigation needs larger samples and process study, such as sub-grid effect



### 3. Development of adjoint radiative transfer model including scattering effect

# Radiative transfer model: PSTAR4

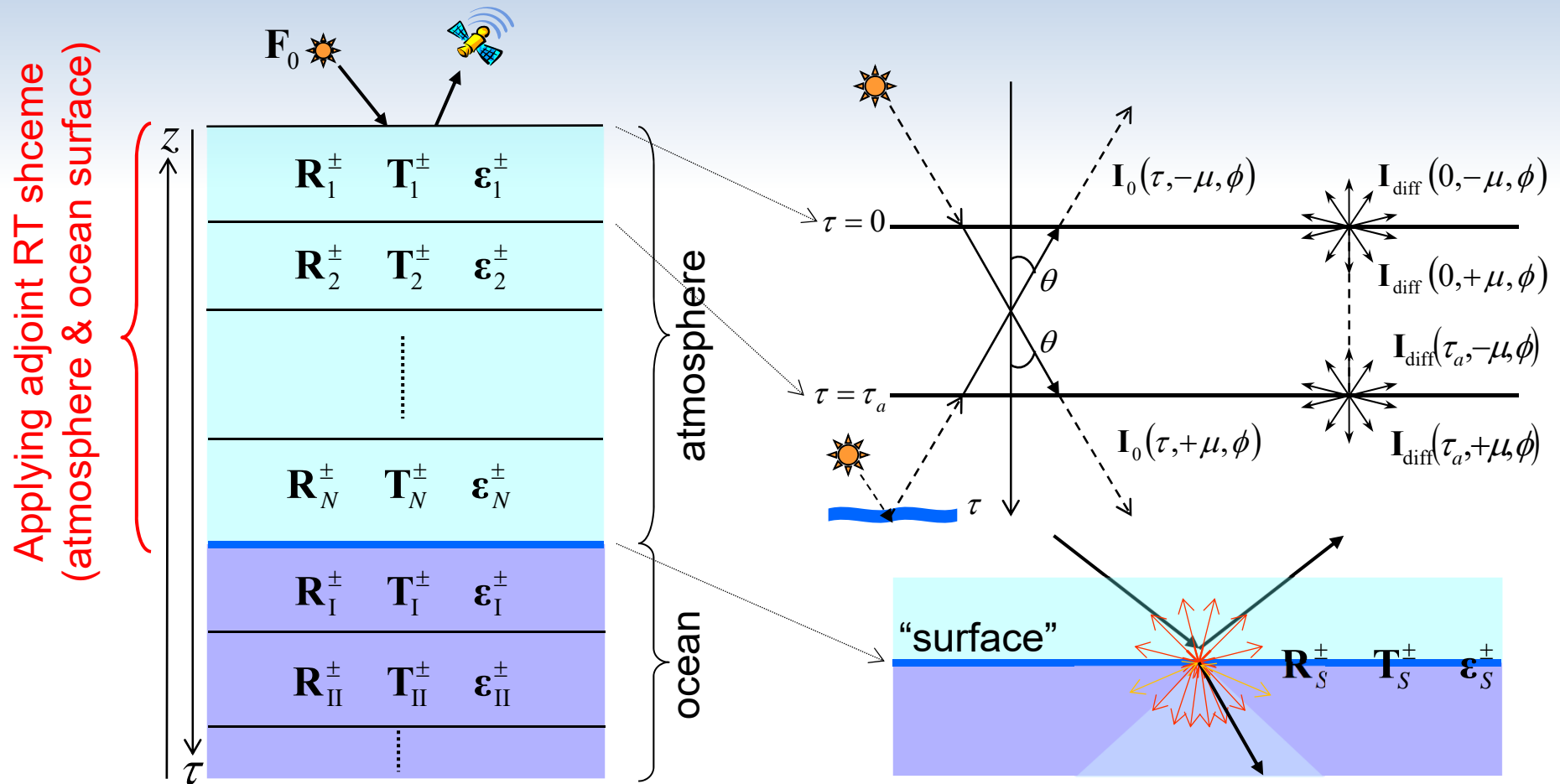
## ◆ Radiative transfer (RT) scheme

- **Vector radiative transfer calculation** of Stokes parameters:  $I$ ,  $Q$ ,  $U$ ,  $V$
- Hybrid RT scheme: **Discrete-ordinate/matrix-operator method** (Ota et al, 2010)
- Coupled atmosphere-ocean system
- Multiple scattering media including thermal sources
- Delta-M truncation method
- Analytical GSF expansion of phase matrix
- Source function integration for angular interpolation (arbitrary viewing geometry)
- Exact single scattering correction: TMS-method (Nakajima and Tanaka, 1988)
- *Rough* or *flat* ocean surface / Lambert surface
- **Adjoint radiative transfer scheme for weighting function calculation**
- Fortran90 code

## ◆ Optical models

- Spherical and spheroidal particle scattering
- Correlated  $k$ -distribution method for narrow band calculation
- Line-by-line calculation using gaseous optical thickness by LBLRTM output
- Wind-roughened ocean surface
- Oceanic water parameterized with chlorophyll-a concentration

# Schematic illustration of PSTAR4's RT scheme



- Reflection, transmission and source matrices ( $\mathbf{R}, \mathbf{T}, \boldsymbol{\epsilon}$ ) for each vertical layer are generated by discrete-ordinate method, and then matrix-operator method is applied to obtain a radiation field of the system.
- The ocean surface is incorporated as a pseudo layer.

# Weighting function (or Jacobian)

Radiance:  $I = I_{\text{dfs}} - I_{\text{TMS}} + I_1 + I_g$

$I_{\text{dfs}}$  : diffused radiance

$I_{\text{TMS}}$  : inaccurate single scattering radiance

$I_1$  : exact single scattering radiance

$I_g$  : sunglint radiance by ocean surface

$I^*$  : adjoint radiance

Weighting function:

$$\frac{\partial I}{\partial p} = \frac{\partial I_{\text{dfs}}}{\partial p} - \frac{\partial I_{\text{TMS}}}{\partial p} + \frac{\partial I_1}{\partial p} + \frac{\partial I_g}{\partial p}$$



Apply adjoint RT

Analytic derivative of single scattering solution

Analytic derivative of sunglint solution

easily can be formulated and implemented

$$W_p = \frac{\partial I}{\partial p} = \langle I^*, \Psi_p \rangle = \int_0^{\tau_0} d\tau \int_{4\pi} d\Omega I^{*T}(\tau, \mu, \phi) \Psi_p(\tau, \mu, \phi)$$

$I_{\text{dfs}}$  : forward RT

$I_{\text{dfs}}^*$  : adjoint RT

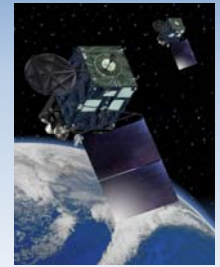
$$W_p = \langle I_{\text{dfs}}^*, \Psi_p \rangle$$

Adjoint RT calculation can be done using the forward RTM.

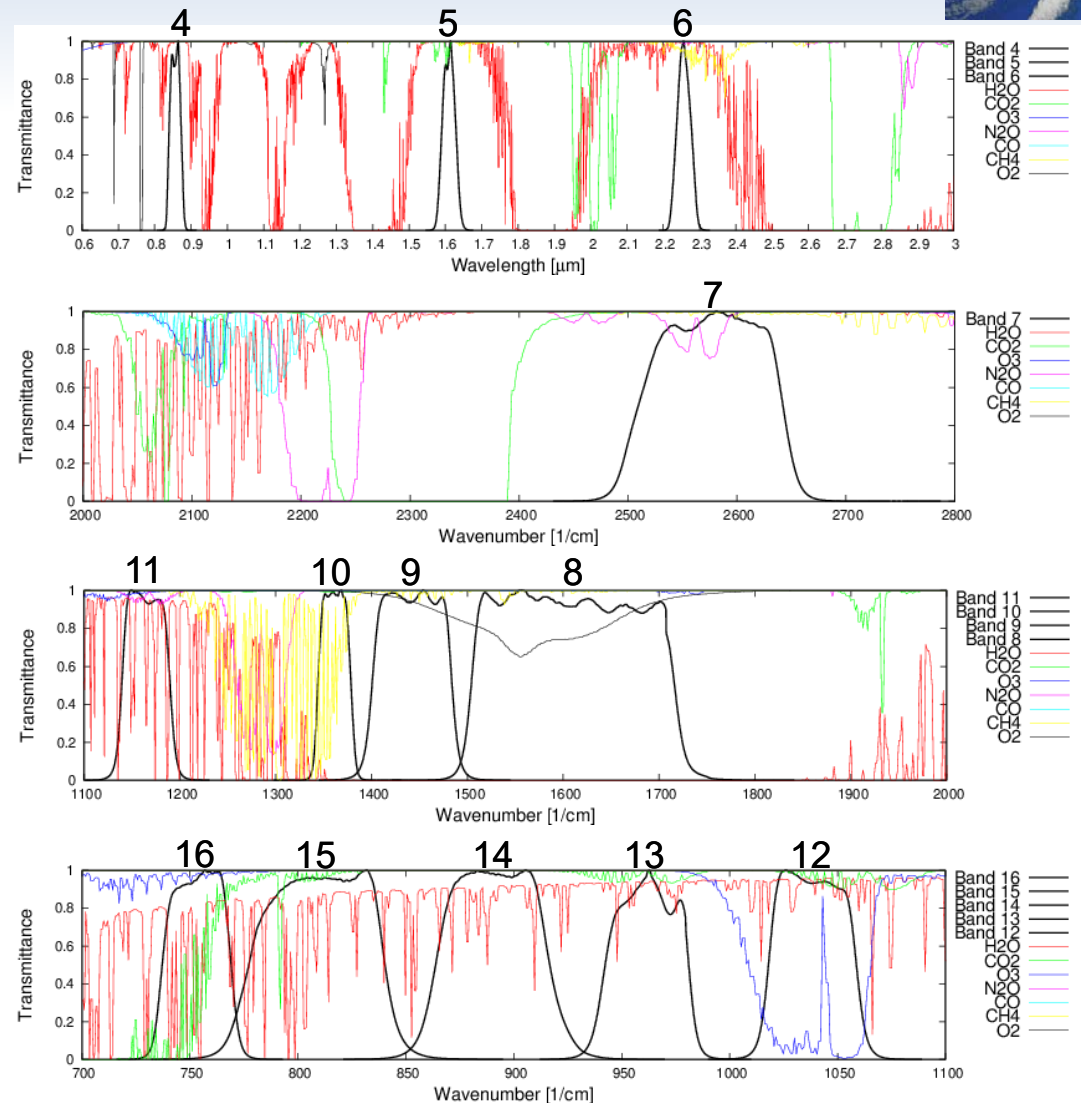
$W_p$  requires:

- Two RT calculations: forward RT ( $I_{\text{dfs}}$ ) and adjoint RT ( $I_{\text{dfs}}^*$ )
- Inner product with linearizing vector  $\Psi_p$  depending on the parameter  $p$  :  $\langle I^*, \Psi_p \rangle$

# Advanced Himawari Imager (AHI) onboard Himawari-8 geostationary satellite



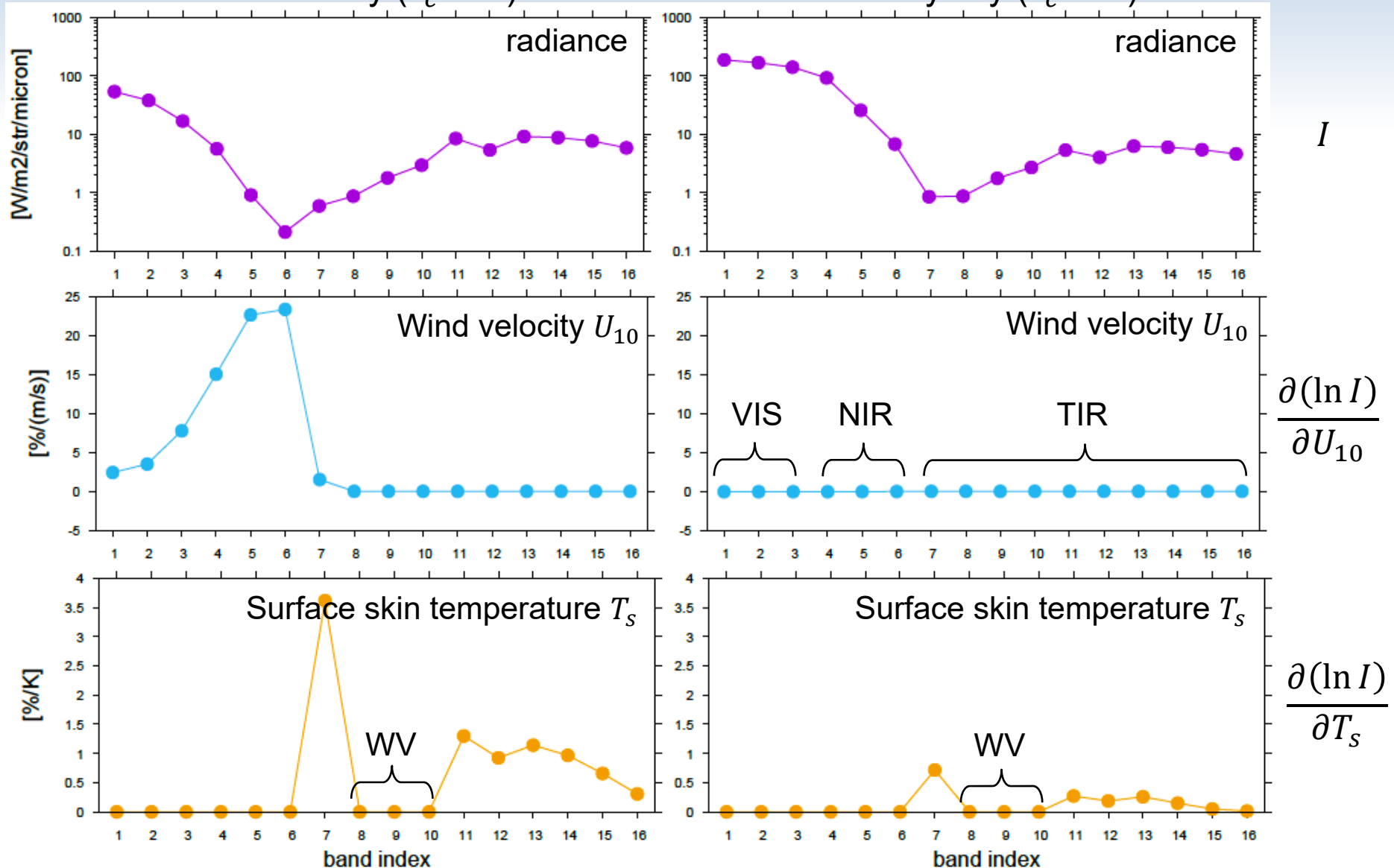
| Band index |     | Central wavelength [μm] | Spatial resolution [km] |
|------------|-----|-------------------------|-------------------------|
| 1          | VIS | 0.47063                 | 1                       |
| 2          |     | 0.51000                 |                         |
| 3          |     | 0.63914                 |                         |
| 4          | NIR | 0.85670                 | 1                       |
| 5          |     | 1.6101                  | 2                       |
| 6          |     | 2.2568                  |                         |
| 7          | TIR | 3.8853                  | 2                       |
| 8          |     | 6.2429                  |                         |
| 9          |     | 6.9410                  |                         |
| 10         |     | 7.3467                  |                         |
| 11         |     | 8.5926                  |                         |
| 12         |     | 9.6372                  |                         |
| 13         |     | 10.4073                 |                         |
| 14         |     | 11.2395                 |                         |
| 15         |     | 12.3806                 |                         |
| 16         |     | 13.2807                 |                         |



# Weighting functions of AHI bands

Clear sky ( $\tau_c = 0$ )

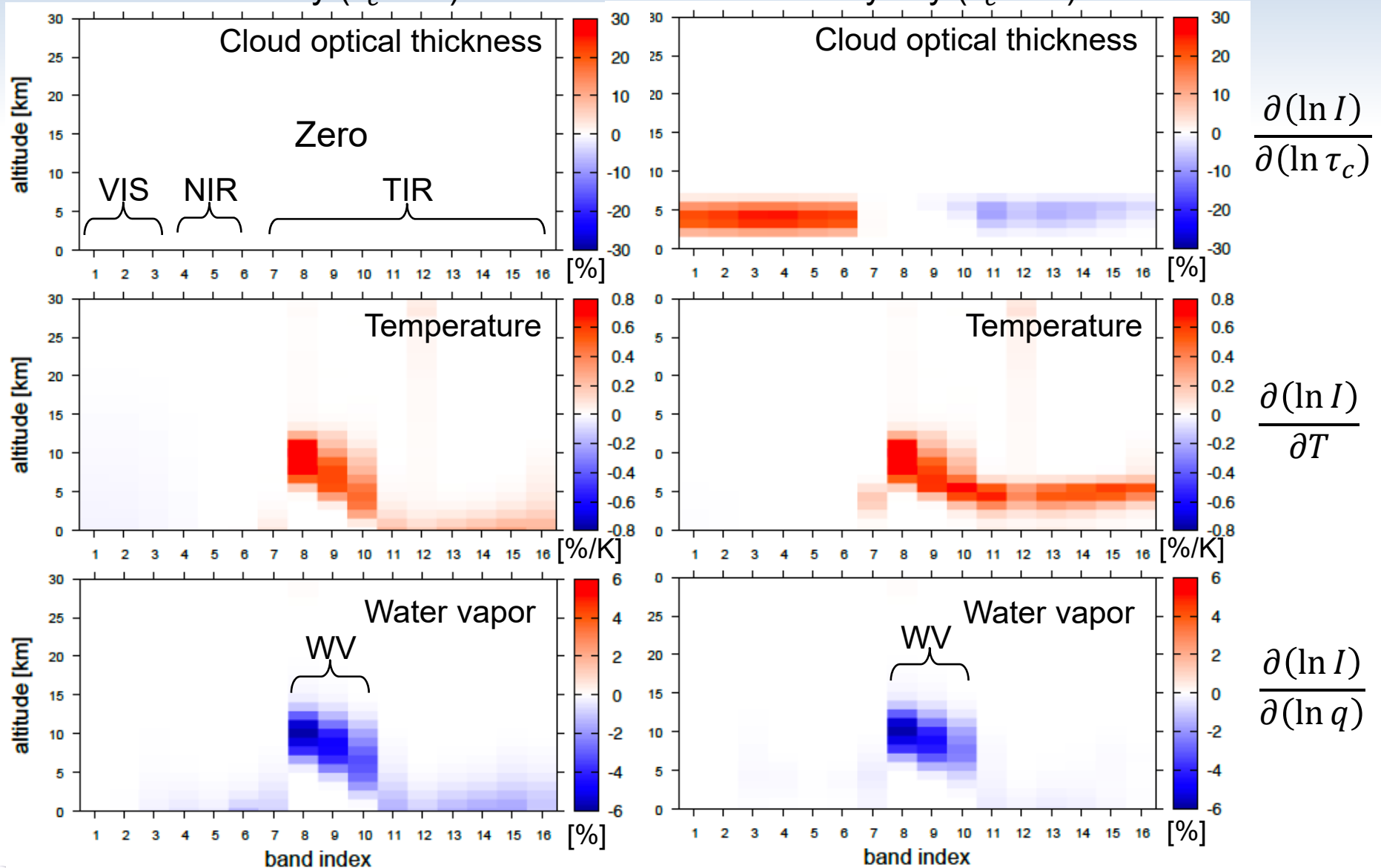
Cloudy sky ( $\tau_c = 5$ )



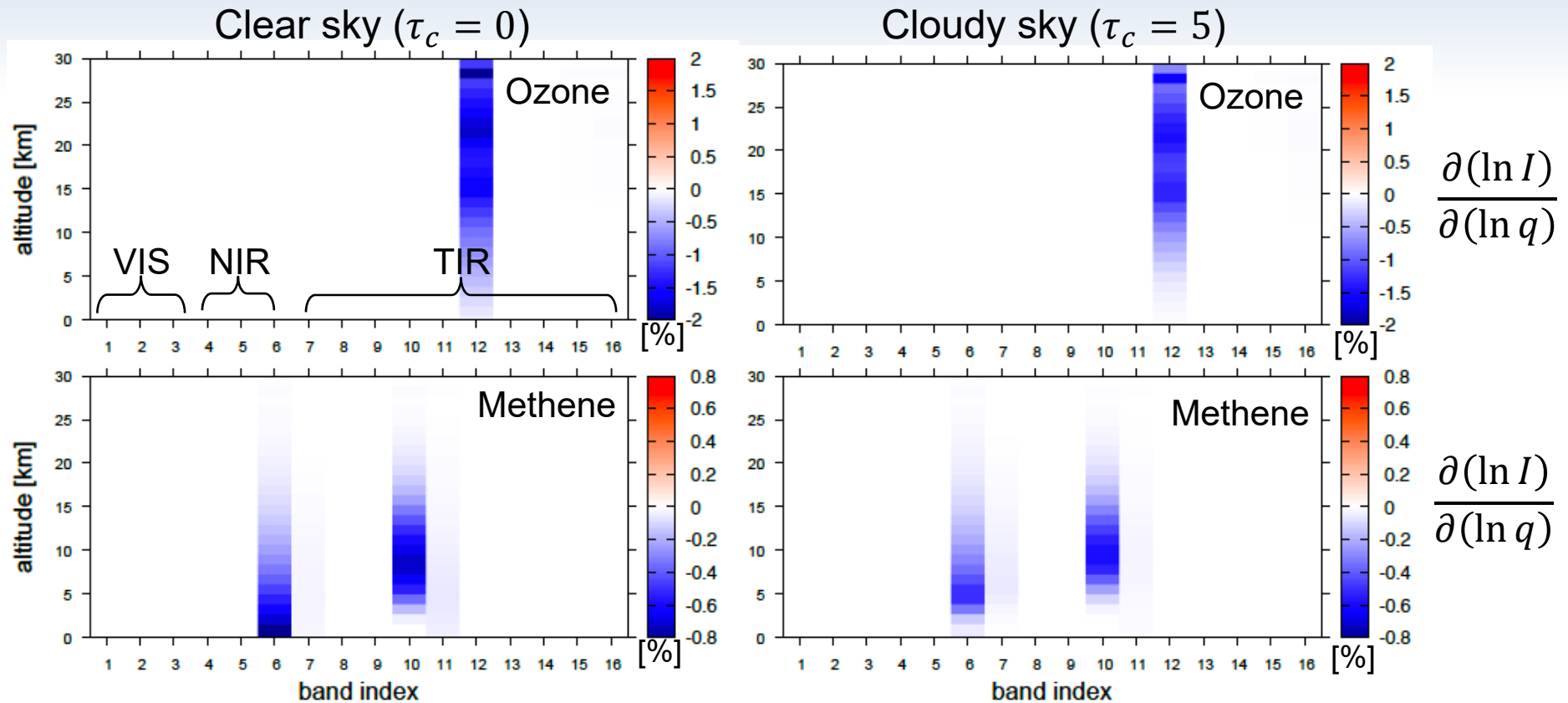
# Weighting functions of AHI band

Clear sky ( $\tau_c = 0$ )

Cloudy sky ( $\tau_c = 5$ )



# Weighting functions of AHI bands





# Summary of topic 3

- ◆ PSTAR4 is a vector RT model for coupled atmosphere–ocean system.
- ◆ The adjoint RT scheme is developed for efficient calculations of weighting functions (Jacobians) with respect to:
  - atmospheric parameters
    - Temperature
    - Gas mixing ratio (water vapor, O<sub>3</sub>, CH<sub>4</sub>, etc.)
    - Cloud/aerosol parameters (optical thickness, SSA, microphysics parameters (beta status))
  - surface parameters
    - Wind velocity  $U_{10}$
    - Surface skin temperature
    - Surface emisivity

# Backup slides

## ◆ Apply JS to Global Spectral Model (GSM)

- Cloud microphysics settings for GSM
  - Conversion of rain/snow flux to mix.ratio
  - Assume PSD and terminal velocity  $V_t$ , which are not defined in GSM
  - Effective radius consistent with radiation scheme
- Subgrid generator
  - Maximum-random overlap assumption, up to 100 columns

# Linearizing vector: $\Psi_p$

- Extinction coefficient ( $\ln k_e$ ):  $\Psi_e(\tau, \Omega) = J(\tau, \Omega) + Q(\tau, \Omega) - I(\tau, \Omega)$
- Absorption coefficient ( $\ln k_a$ ):  $\Psi_a(\tau, \Omega) = [1 - \omega(\tau)][B(\tau)\mathbf{E}_1 - I(\tau, \Omega)]$
- Single scattering albedo ( $\ln \omega$ ):  $\Psi_\omega(\tau, \Omega) = J(\tau, \Omega) - \omega(\tau)B(\tau)\mathbf{E}_1$

$$J(\tau, \Omega) = \omega(\tau) \int_{4\pi} \mathbf{Z}(\tau, \Omega, \Omega') I(\tau, \Omega) d\Omega'$$

$$\mathbf{E}_1 = [1, 0, 0, 0]^T$$

- Atmospheric Planck function ( $B(T)$ ):  $\Psi_B(\tau, \Omega) = [1 - \omega(\tau)]\mathbf{E}_1$
- Ground surface Planck function ( $B(T_s)$ ):  $\Psi_{BS}(\tau, \Omega) = \psi_b(\tau, -\mu)\epsilon\mathbf{E}_1$   
( $\epsilon$ : ground surface emissivity)

- Wind velocity over the ocean ( $u_{10}$ ):

$$\Psi_{u_{10}}(\tau, \Omega) = \psi_b(\tau, -\mu) \int_{\Omega_+} \frac{\partial \mathbf{R}(\Omega, \Omega')}{\partial u_{10}} I(\tau_0, \Omega') \mu' d\Omega'$$

( $\mathbf{R}(\Omega, \Omega')$ : Ocean surface reflection function)

# Application of WF calculation to AHI bands

## Simulation settings

- ◆ RT model: PSTAR4
  - ✓ Discrete ordinate method (12 streams)
  - ✓ Forward-adjoint RT method
- ◆ Wavelength: Advanced Himawari Imager (AHI) 16 bands, on Himawari-8
- ◆ Atmospheric profile: Mid-latitude summer (49 layers, 0-120 km)
  - ✓ HITRAN2012: 7 major molecules (H<sub>2</sub>O, CO<sub>2</sub>, O<sub>3</sub>, N<sub>2</sub>O, CO, CH<sub>4</sub>, O<sub>2</sub>)
  - ✓ Correlated *k* distribution (CKD) method for gas absorption coefficient
- ◆ Water cloud: COT 5.0 @ wavelength 0.5μm
  - ✓ Log-normal particle size distribution (mode radius 8μm)
- ◆ No aerosol loading
- ◆ Rough ocean surface: U10 = 7m/s, Tg = 300 K

# Optical properties of each AHI bands

